JOURNAL OF APPLIED ELECTROCHEMISTRY **27** (1997) 953–958

$Li_{1-x}Na_xV_3O_8$ as positive materials for secondary lithium batteries

N. KUMAGAI, A. YU
Department of Applied Chemistry and Molecular Science, Faculty of Engineering, Iwate University, Morioka, 020 Japan

K. WEST
Department of Physical Chemistry, The Technical University of Denmark, DK-2800, Lyngby, Denmark

Received 30 July 1996; revised 25 November 1996

A series of $Li_{1-x}Na_xV_3O_8$ ($0 < x < 1$) solid solution were investigated as positive materials for secondary lithium batteries. The materials were characterized by X-ray diffraction and infrared spectrum measurements, showing that pure phases of $Li_{1-x}Na_xV_3O_8$ were formed with the same monoclinic structure as LiV_3O_8. The electrochemical characteristics including charge–discharge characteristics were compared with those of LiV_3O_8 and NaV_3O_8, showing that the $Li_{0.7}Na_{0.3}V_3O_8$ electrode shows the best electrochemical performance among several $Li_{1-x}Na_xV_3O_8$; at a current density of $0.2\,mA\,cm^{-2}$, it gave a discharge capacity of $215\,mAh\,g^{-1}$-oxide which was about 80% of the theoretical discharge capacity. The cathode current loading test also showed that $Li_{1-x}Na_xV_3O_8$ has the advantage of both LiV_3O_8 and NaV_3O_8. Furthermore, the thermodynamics and kinetics of lithium intercalation into the oxide structure were also examined.

1. Introduction

Some vanadium oxides, V_2O_5 and V_6O_{13}, have been investigated as promising cathode materials for ambient temperature secondary lithium batteries [1]. The layered trivanadate, LiV_3O_8 [2], which has received remarkable attention as an alternative for V_6O_{13}, has been used as a positive electrode in these batteries. A great deal of work has been done, including preparation and intercalation chemistry, and the results [3–5] have shown that preparation methods of the oxides strongly influence their electrochemical properties.

Recently, MV_3O_8 (M = Na or K) as cathode materials for secondary lithium batteries have been first reported by Pistoia *et al.* [6, 7]. The presence of the other alkali metals such as Na and K gives the advantage of large interlayer distance than that of LiV_3O_8. These materials have also been tested as positive materials for sodium and magnesium batteries [8, 9].

NaV_3O_8 with a monoclinic structure [6] showed a higher value of chemical diffusion coefficient of lithium and good cycling performance with a higher charge–discharge efficiency. However, the discharge capacity and discharge voltage were somewhat lower than those of LiV_3O_8, leading to lower energy density. Therefore, it is expected that partial substitution of lithium ion in LiV_3O_8 with sodium ion having large ionic radius, $Li_{1-x}Na_xV_3O_8$ ($0 < x < 1$), could lead to a higher diffusion coefficient of lithium in the structure and a larger discharge capacity. In the present study mixed Li/Na vanadates, $Li_{1-x}Na_xV_3O_8$ ($0 < x < 1$), were investigated as positive materials for lithium secondary batteries and the results are compared with those of LiV_3O_8 and NaV_3O_8.

2. Experimental details

$Li_{1-x}Na_xV_3O_8$ compounds of different x values were formed by heating mixtures of V_2O_5, Na_2CO_3 and Li_2CO_3 (reagent grade, Kanto Chemical Co.) in different molar ratios. The mixture was well mixed in a porcelain crucible and heated to 620 °C with a heating of 1 °C min^{-1} in air using a SCM-200 type electric furnace (Sibata Co.) and kept for 6 h at the same temperature. The heated compounds were quenched to room temperature and then ground in an agate mortar.

The compounds were characterized by the X-ray diffraction(XRD) method and infrared spectroscopy. XRD measurements were performed using a Rigaku Denki Geigerflex 20B with CuK_α line and infrared spectrum were recorded on a Hitachi 295IR spectrophotometer with a KBr disc method.

The electrode and cell preparation have been described previously [10]. The mixture of the product and graphite as a conducting agent, in a weight ratio of 1:1, was compressed on a nickel net under about 50 MPa pressure and the pellet thus obtained was used as working electrode after drying under vacuum at 25 °C for 1 d. Typical positive electrode loadings were about $10\,mg\,cm^{-2}$(active material). The electrolyte used was 1 M PC(propylene carbonate)/$LiClO_4$ solution and lithium pellets were used both as the reference and the counter electrodes. The investiga-

tion was undertaken using a glass beaker type cell at room temperature in a dry box under an argon atmosphere. A.c. impedance measurements were performed by using NF Electronic Instrument 5720B frequency response analyzer, Tohogiken potentiostat 2000 and HP 9000-200 microcomputer. A 5 mV r.m.s. perturbation was supplied in the frequency range from 63 kHz to 1 mHz and the results are presented in the complex impedance plane.

3. Results and discussion

The X-ray diffraction patterns of $Li_{1-x}Na_xV_3O_8$ with different x values are given in Fig. 1. The diffraction patterns of $Li_{1-x}Na_xV_3O_8$ are very similar to those of LiV_3O_8 and NaV_3O_8, but the diffraction peaks appear at different angles, related to the substitution of Li with Na. In all the products, it is observed that the position (2 Θ) of the (1 0 0) diffraction peaks lie between 13° and 14° and the (1 0 0) peak shifts to smaller 2 Θ angle with an increase in Na content. As shown in Fig. 2, a continuous increase in the interlayer distance, d_{100}, is brought about by substitution of Li with Na. This shows that the presence of Na^+ ($r = 1.0$ Å) between the layers fixed the d_{100} value larger than that of Li^+ ($r = 0.7$ Å). The XRD patterns also show that a series of $Li_{1-x}Na_xV_3O_8$ solid solution are formed as single phase compounds over the range $0 < x < 1$.

Typical infrared spectra of $Li_{0.7}Na_{0.3}V_3O_8$ compared with LiV_3O_8 and NaV_3O_8 are shown in Fig. 3. All the infrared responses showed absorption bands at 1020, 960 and 760 cm^{-1}, which are assigned to the V═O and V—O—V vibrations [11]. No other obvious infrared absorption bands were observed, showing the formation of pure phase compounds from heating the starting mixtures.

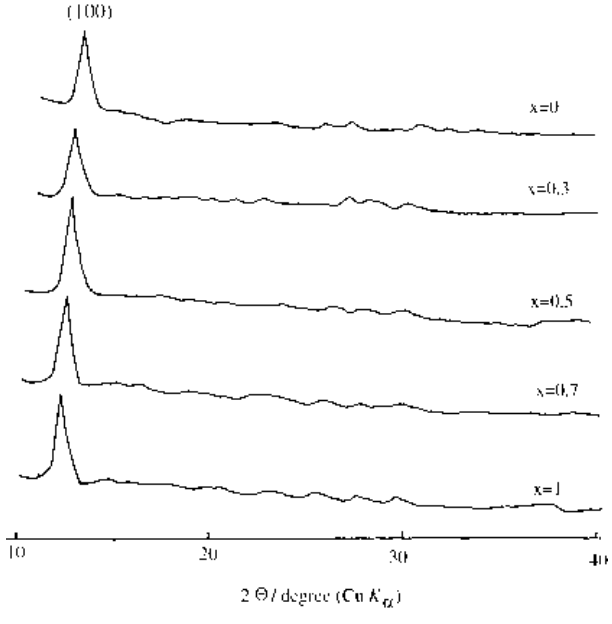

Fig. 1. XRD patterns for $Li_{1-x}Na_xV_3O_8$ prepared at 600 °C.

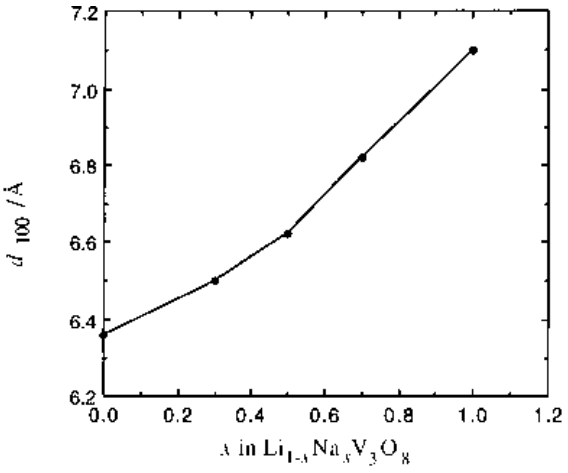

Fig. 2. Variation in d_{100} values as a function of x in $Li_{1-x}Na_xV_3O_8$.

The SEM photograph of $Li_{0.7}Na_{0.3}V_3O_8$ is shown in Fig. 4. The product consists of fine particles with a needle-like shape of 1–5 μm in section.

A typical cyclic voltammogram of a $Li_{0.7}Na_{0.3}V_3O_8$ electrode is shown in Fig. 5, compared with those of LiV_3O_8 and NaV_3O_8 electrodes. These voltammograms were measured at a sweep rate of 0.3 mV s^{-1} in the potential range 3.8 V to 1.7 V at 25 °C. The open circuit potential of $Li_{0.7}Na_{0.3}V_3O_8$ is 3.7 V vs Li/Li^+. In the cyclic voltammograms upon cycling (b), three cathodic peaks are observed at potentials of 2.3, 2.5 and 3.2 V and two anodic peaks at 2.8 V and 3.6 V. The several CV peaks suggest that lithium can occupy several different sites of the host structure. As also seen from Fig. 5, the cyclic voltammetric behaviour of the $Li_{0.7}Na_{0.3}V_3O_8$ electrode is similar to that of LiV_3O_8 and NaV_3O_8, suggesting that $Li_{0.7}Na_{0.3}V_3O_8$

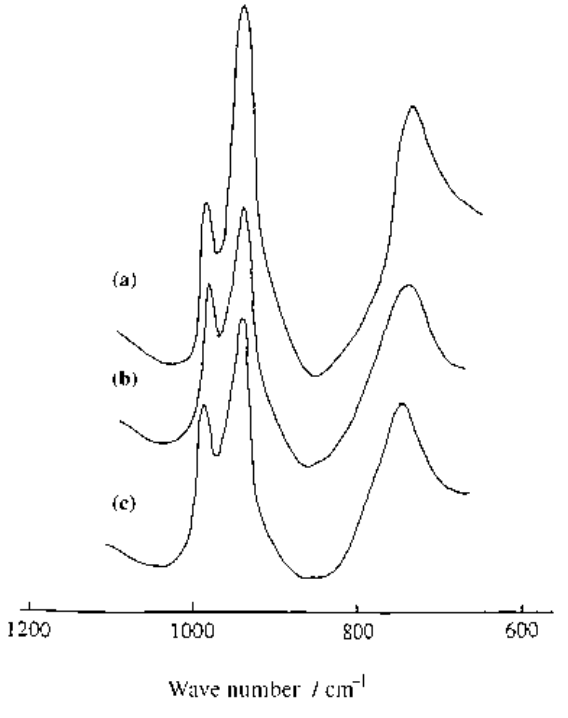

Fig. 3. Infrared spectra of $Li_{1-x}Na_xV_3O_8$. (a) LiV_3O_8, (b) $Li_{0.7}Na_{0.3}V_3O_8$, (c) NaV_3O_8.

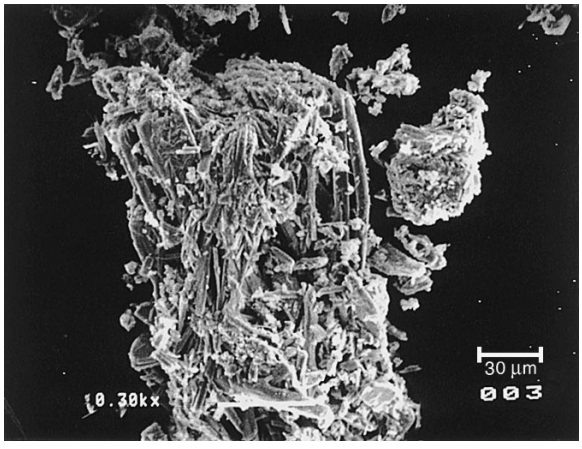

Fig. 4. SEM photograph of $Li_{0.7}Na_{0.3}V_3O_8$.

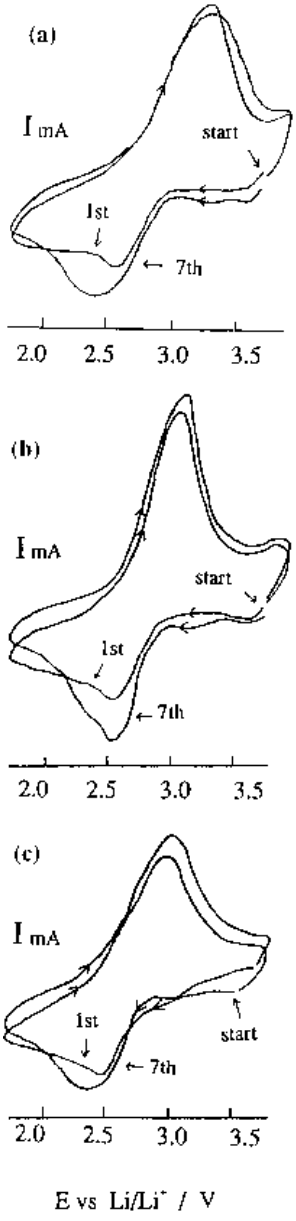

Fig. 5. Cyclic voltammograms of several vanadates at 25 °C. (a) LiV_3O_8, (b) $Li_{0.7}Na_{0.3}V_3O_8$, (c) NaV_3O_8. Scanning rate: 0.3 mV s^{-1}.

has similar electrochemical behaviour as a positive electrode for secondary lithium batteries. However, the peak current density of $Li_{0.7}Na_{0.3}V_3O_8$ is higher than that of the others at the same experimental condition, suggesting that the Li/Na mixed compound shows a better electrode performance. The cyclic voltammogram show a good reversibility at a sweep rate of 0.3 mV s^{-1} and almost the same curve was observed during 2–7 cycles, suggesting that the incorporation of lithium into the host lattice occurs without destroying its original structure.

Typical initial discharge curves of $Li_{1-x}Na_xV_3O_8$ electrodes with different x values, measured at a current density of 0.2 mA cm^{-2} at potentials down to 1.7 V vs Li/Li^+ in 1 M $LiClO_4$–PC solution at 25 °C, are shown in Fig. 6. The discharge curves show an average discharge potential of about 2.6 V in $Li_{0.8}Na_{0.2}V_3O_8$ and the average potential decreases with an increase in sodium content. The discharge potential is mainly decided by the site energy of intercalated lithium atoms. In LiV_3O_8, an average Li—O bond length is about 2.17 Å [12], and for NaV_3O_8, similar to that of $Na_2V_6O_{13}$, the Na—O bond length is about 2.5 Å [13]. A larger bond length may produce weaker interaction between the intercalated lithium atoms and the host structure, so that the substitution of lithium by sodium in LiV_3O_8 leads to a decrease in the site energies available to the incorporated lithium atoms. Indeed, the discharge potential decreased with increase in Na content. As seen in Fig. 6, $Li_{0.7}Na_{0.3}V_3O_8$ gives the highest discharge capacity of 215 mAh g^{-1} (related to the active material) corresponding to 2.4 e^- mol^{-1}. This capacity is about 80% of the theoretical one (3 e^- mol^{-1}) and the energy density is about 600 Wh kg^{-1}.

To see how the sodium content in the vanadates, x value, affects their electrode behaviour in secondary lithium batteries, the vanadates were charge–discharge cycled in the potential range 3.8 V to 1.7 V with a current density of 0.2 mA cm^{-2} at 25 °C. In Fig. 7, the discharge capacity during 40 cycles are shown as a

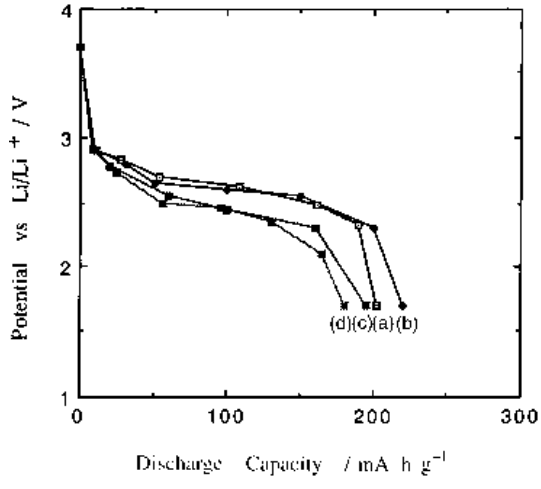

Fig. 6. Initial discharge curves for various $Li_{1-x}Na_xV_3O_8$ at 25 °C. (a) $x = 0.2$, (b) $x = 0.3$, (c) $x = 0.5$. (d) $x = 0.7$. Current density: 0.2 mA cm^{-2}.

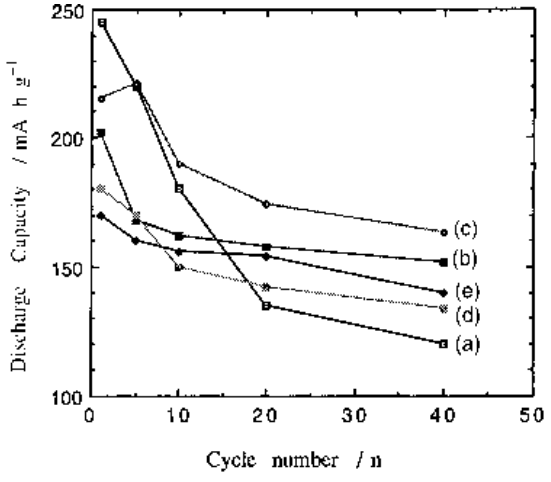

Fig. 7. Discharge capacity as a function of cycle number (a) LiV_3O_8, (b) $Li_{0.8}Na_{0.2}V_3O_8$, (c) $Li_{0.7}Na_{0.3}V_3O_8$, (d) $Li_{0.3}Na_{0.7}V_3O_8$, (e) NaV_3O_8. Charge–discharge current density: 0.2 mA cm^{-2}.

function of cycle number. The $Li_{0.7}Na_{0.3}V_3O_8$ electrode shows the highest discharge capacity without large capacity loss with cycling.

To evaluate the effect of depth of lithium intercalation into the host structure, XRD diagrams of $Li_n[Li_{0.7}Na_{0.3}V_3O_8]$ are shown in Fig. 8, at different depths of lithium intercalation. Because of the weak XRD response of the discharge products, the figure only gives the different peak at $2\Theta \simeq 14°$. As seen from Fig. 8, the d_{100} diffraction peak shifts to a smaller angle at $n \leq 1.5$. At $n = 1.5$, the peak was observed at the lowest position, while $n > 1.5$, the peak shifts to a higher 2Θ position with increasing intercalation depth of lithium. This phenomenon is probably brought about by replacing the sodium atoms of the vanadate with electrochemically intercalated lithium atoms. However, when the original $Li/Li_{0.7}Na_{0.3}V_3O_8$ cell was charged, the cell voltage quickly rose to 4.5 V at a current density of 0.2 mA cm^{-2}, giving little charge capacity less than 5 mAh g^{-1}. This fact suggests that the Na atom is firmly bound to the oxide matrix, so that the sodium atom is not substituted by intercalated lithium atom and the original structure is very stable during cycling.

The XRD diagram and infrared response showed that $Li_{0.7}Na_{0.3}V_3O_8$ has a structure similar to that of LiV_3O_8 [13], therefore the structure can be shown as in Fig. 9. It retains a monoclinic structure and the space group in $P2_1/m$. The structure consists of VO_6 octahedra and VO_5 distorted trigonal bipyramids and is built up by sharing the edges and corners of the trigonal bipyramids and the octahedra to form a zigzag ribbon. Lithium can be localized in both of two kinds of vacant sites named octahedral and tetrahedral sites (Fig. 9), in which the original combined lithium atoms occupy octahedral coordinated sites and the intercalated ones occupy tetrahedral sites, respectively. With lithium intercalation into the original monoclinic lattice at $n \leq 1.5$, a small expansion in the a_0-lattice parameter, about 6% occurs as shown in Fig. 8. On the other hand, at $x > 1.5$, the diffraction peak at $2\Theta \simeq 14°$ shifts to a higher angle, which is probably due to the formation of new phase. This phenomenon is like that for LiV_3O_8 as observed by Pistoia and Thackery *et al.* [14, 15]; at $x > 1.5$, the Li^+ ions in the octahedral sites are displaced by the incoming lithium ions into neighbouring octahedral sites. This displacement, which is accomplished by a shortening of the V—O bond distances due to the reduction of vanadium ions, modifies the oxygen–ion array towards a cubic-close-packing, generating a defect rock salt phase.

Such a structural variation with lithium intercalation can also be observed from the OCV–*n* curve of the $Li/Li_{0.7}Na_{0.3}V_3O_8$ cell shown in Fig. 10. As seen in this figure, the OCV–*n* curve gives a large potential drop at the initial stage, followed by a gradual decrease in the OCV in the *n*-value range from 0.5 to 1.5. This reveals the formation of a single phase during lithium intercalation. At $n > 1.5$, the OCVs just remain at 2.55 V. This suggests a two-phase coexistence, which is coincident with the XRD observation. When the OCV curve is compared with that of LiV_3O_8 [14], the potential at the plateau is somewhat lower than that of LiV_3O_8 (2.62 V), also reflecting a lower site energy of the intercalated lith-

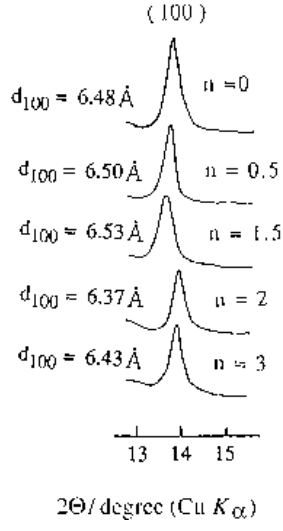

Fig. 8. XRD diagrams of $Li_n[Li0_{0.7}Na_{0.3}V_3O_8]$ at different depths of lithium intercalation.

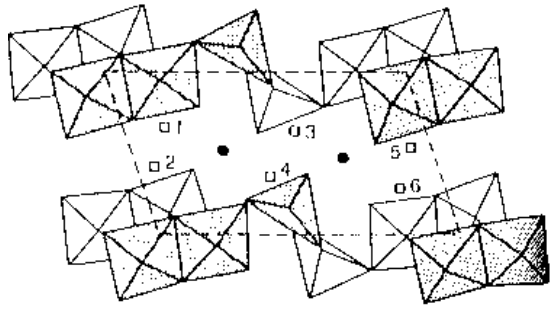

Fig. 9. Structure model of LiV_3O_8. Key:(●) octahedral and (□) tetrahedral.

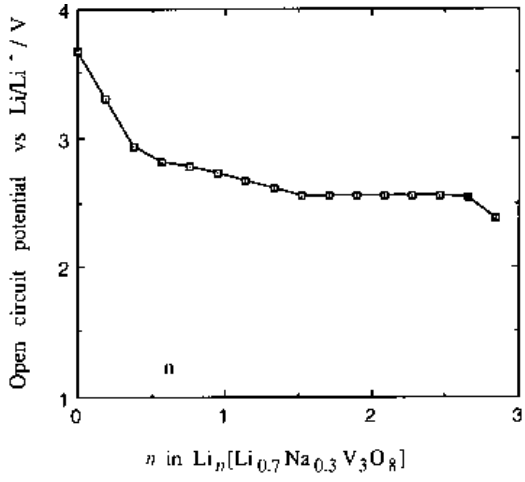

Fig. 10. OCV–n curve of Li/Li$_n$[Li$_{0.7}$Na$_{0.3}$V$_3$O$_8$] cell at 25 °C.

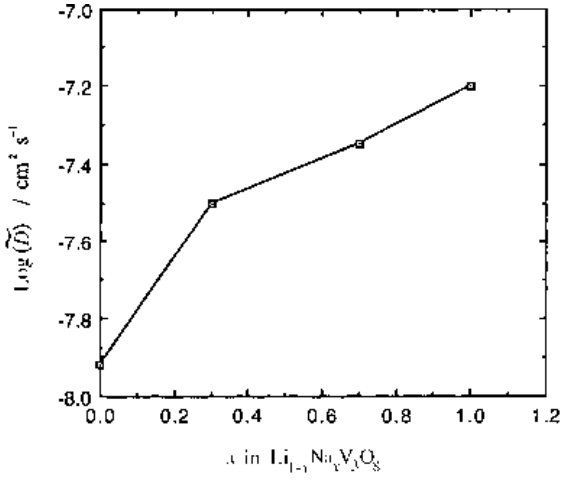

Fig. 12. Chemical diffusion coefficient as a function of x value in Li$_n$[Li$_{1-x}$Na$_x$V$_3$O$_8$] with the n value of 0.2 at 25 °C.

ium atoms as discussed above. The standard free energies, ΔG_I°, for lithium intercalation into oxides are given by following equation:

$$\Delta G_I^\circ = \int_0^n E(n)\mathrm{d}n \quad (1)$$

where $E(n)$ is the open circuit potential at the n value. The calculated values, ΔG_I°, are about 335 kJ mol^{-1} at $n = 1$ and 604 kJ mol^{-1} at $n = 2$ in Li$_n$[Li$_{0.7}$Na$_{0.3}$V$_3$O$_8$].

To evaluate the effect of the substitution of lithium with sodium in LiV_3O_8 on the rate capacity, $Li_{0.7}Na_{0.3}V_3O_8$ was submitted to discharge at various current densities. The discharge capacities of the $Li_{0.7}Na_{0.3}V_3O_8$ electrode at the 5th cycling, compared with those of LiV_3O_8 and NaV_3O_8, are shown in Fig. 11 as a function of current density. $Li_{0.7}Na_{0.3}V_3O_8$ shows better capacity retention, and even at a high current density of 5 mA cm^{-2}, the capacity of 115 mAh g^{-1} could still be recovered.

A typical a.c. impedance spectrum of a Li$_{0.2}$[$Li_{0.7}Na_{0.3}V_3O_8$] electrode contained a semicircle at a low frequency and a spike with a phase angle of about 45° at high frequency. Using the method discussed by Ho and Weppner [16, 17], the chemical diffusion coefficient, $\tilde{D}$, of the electroactive species in the electrode is given by the following equations:

$$|Z_\omega| = A_\omega \omega^{-1/2} \quad (2)$$

$$A_\omega = V_m(\mathrm{d}E/\mathrm{d}n)/Fa\tilde{D}^{1/2} \quad (3)$$

where V_m(35.6 cm^3) is the molar volume of the electrode material. dE/dn is the slope of the thermodynamic curve (OCV–n curve), Z_ω is the Warburg impedance, a is the electroactive surface area of the electrode (a geometric area of 1.4 cm^2 is used in this study). The chemical diffusion coefficients of lithium were deduced from the a.c. impedance spectra and the coefficients are shown in Fig. 12 as a function of sodium content at the same depth of lithium intercalation, $n = 0.2$. The $\tilde{D}$ value for LiV_3O_8, $Li_{0.7}Na_{0.3}V_3O_8$ and NaV_3O_8 at an intercalation depth of lithium of $n = 0.2$, are of the order of 1.3×10^{-8} cm^2 s^{-1}, 3.1×10^{-8} cm^2 s^{-1} and 6.6×10^{-8} cm^2 s^{-1} at 25 °C, respectively. The substitution of lithium with sodium enhances the chemical diffusion coefficient, which may be related to larger interlayer spacing of the vanadates.

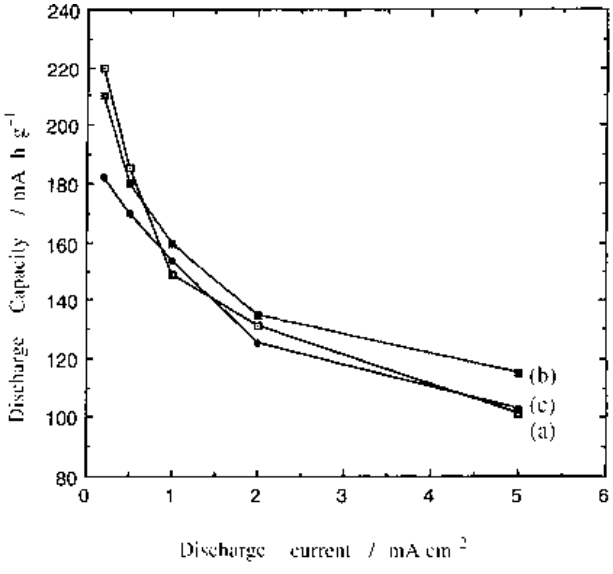

Fig. 11. Discharge capacity at the 5th cycle as function of current density. (a) LiV_3O_8, (b) $Li_{0.7}Na_{0.3}V_3O_8$, (c) NaV_3O_8.

4. Conclusion

The single phase materials, $Li_{1-x}Na_xV_3O_8$ ($0 < x < 1$), can be formed by substitution of lithium with sodium in LiV_3O_8, leading to high discharge capacity, high cyclability and high rate capability for use as positive material for secondary lithium batteries. The $Li_{0.7}Na_{0.3}V_3O_8$ composition material gave a discharge capacity of 215 mAh g^{-1}, which is above 80% of the theoretical value. The chemical diffusion coefficient is of the order of 10^{-8} cm^2 s^{-1} at 25 °C, higher than that of LiV_3O_8.

Thermodynamic studies of lithium insertion into the $Li_{0.7}Na_{0.3}V_3O_8$ electrode reveal that at $x \leq 1.5$, the potential decreases linearly with an increase in depth of lithium intercalation and at $x > 1.5$, it is

stable at 2.55 V; this can be related to the variation in the original structure with lithium intercalation.

Acknowledgement

The authors thank N. Kumagai and S. Saito for their help with the experimental work.

References

[1] N. Kumagai and K. Tanno, *Denki Kagaku* **48** (1980) 432.
[2] G. Pistoia, M. Pasquali, G. Wang and L. Li, *J. Electrochem. Soc.* **137** (1990) 2365.
[3] J. O. Besenhard and R. Schollhorn, *J. Power Sources* **1** (1976/77) 267.
[4] K. West, B. Zachau-Christiansen, M. J. L. Qstergard and T. Jacobsen, *ibid.* **20** (1987) 165.
[5] K. Takei, N. Tarada, K. Ishihara, T. Iwahori and T. Tanaka, *Ext. Abstr.*, The Electrochemical Soc., **91–2** (44) (1991).
[6] M. Pasquali and G. Pistoia, *Electrochimi Acta* **36** (1991) 1549.
[7] G. Pistoia, G. Wang and D. Zane, *Solid State Ionics* **76** (1995) 285.
[8] P. Novak, W. Scheifele, F. Joho and O. Haas, *J. Electrochem. Soc.* **142** (1995) 2544.
[9] G. Wang and G. Pistoia, *J. Electroanal. Chem.* **302** (1991) 275.
[10] N. Kumagai, S. Tanifuji, T. Fujiwara and K. Tanno, *Electrochim. Acta* **37** (1992) 1039.
[11] Y. Kera, *J. Solid State Chem.* **51** (1984) 205.
[12] K. M. Abraham and M. Alamgier, *J. Electrochem. Soc.* **137** (1990) 1657.
[13] A. D. Wadsley, *Acta Cryst*. **10** (1957) 261.
[14] G. Pistoia, M. Pasquali and M. Tocci, *J. Electrochem. Soc.* **132** (1985) 281.
[15] L. A. de Piccitto, K. T. Adendorff, D. C. Liles and M. M. Thackeray, *Solid State Ionics* **62** (1993) 297.
[16] C. Ho, I. D. Raistric and R. A. Huggins, *J. Electrochem. Soc.* **127** (1980) 269.
[17] W. Weppner, R. A. Huggins, *Ann. Rev. Mat. Sci.* **8** (1978) 269.